

# High positive carbonate carbon isotope excursion identified in the North China Craton: Implications for the Lomagundi–Jatuli Event

Shuan-Hong Zhang<sup>1,2</sup> | Hong-Yu Wang<sup>1</sup> | Hao-Shu Tang<sup>3</sup> | Yu-Hang Cai<sup>4</sup> | Ling-Hao Kong<sup>1</sup> | Jun-Ling Pei<sup>2,5</sup> | Qi-Qi Zhang<sup>1,2</sup> | Guo-Hui Hu<sup>1,2</sup> | Yue Zhao<sup>1,2</sup>

<sup>1</sup>SinoProbe Laboratory, Institute of Geomechanics, Chinese Academy of Geological Sciences, Beijing, China

<sup>2</sup>Key Laboratory of Paleomagnetism and Tectonic Reconstruction, Ministry of Natural Resources, Beijing, China

<sup>3</sup>State Key Laboratory of Ore Deposit Geochemistry, Institute of Geochemistry, Chinese Academy of Sciences, Guiyang, China

<sup>4</sup>School of Earth Sciences, Yunnan University, Kunming, China

<sup>5</sup>School of Earth Sciences, East China University of Technology, Nanchang, China

## Correspondence

Shuan-Hong Zhang, SinoProbe Laboratory, Institute of Geomechanics, Chinese Academy of Geological Sciences, Beijing 100081, China.

Email: [tozhangshuanhong@163.com](mailto:tozhangshuanhong@163.com)

## Funding information

National Natural Science Foundation of China, Grant/Award Number: 41920104004, 41725011 and U2244213

## Abstract

Records of the Lomagundi–Jatuli Event (LJE) are well preserved globally, but high  $\delta^{13}\text{C}_{\text{carb}}$  carbonates have not been identified in the North China Craton (NCC). Our results on ~3–4 km thick carbonates from the newly confirmed Palaeoproterozoic successions in Fanhe Basin in the northeastern NCC show that the ~2.20–2.06 Ga carbonates have positive carbon isotope excursion and those deposited after 2.06 Ga have normal carbon isotope. Specially, carbonates from the Daposhan Formation have  $\delta^{13}\text{C}_{\text{carb}}$  values of 10.2‰–11.8‰, which is the largest positive carbon isotope excursion in the NCC. The ~2.20–2.06 Ga carbonates in Fanhe Basin have similar  $\delta^{13}\text{C}_{\text{carb}}$  values as those contemporaneously deposited in other cratons and their  $\delta^{13}\text{C}_{\text{carb}}$  values exhibit a decreasing trend from ~2.20 Ga to 2.06 Ga. Our identification of carbonates with high positive  $\delta^{13}\text{C}_{\text{carb}}$  values in Fanhe Basin not only casts new lights on records of the LJE in the NCC, but also provides important constraints on global significance of the positive  $\delta^{13}\text{C}_{\text{carb}}$  excursion of LJE.

## KEY WORDS

carbon isotope excursion, Great Oxidation Event (GOE), Lomagundi–Jatuli Event (LJE), marine carbonate, North China Craton (NCC)

## 1 | INTRODUCTION

The Great Oxidation Event (GOE) started from 2.43 Ga (Gumsley et al., 2017) or 2.33–2.32 Ga (Bekker et al., 2004; Luo et al., 2016; Poulton et al., 2021) is a profound turning point in Earth's history and represents the first significant buildup in Earth's atmospheric oxygen (Canfield, 2005; Holland, 1999, 2002, 2009; Konhauser et al., 2009; Kump, 2008; Lyons et al., 2014). It was followed by Earth's largest known positive  $\delta^{13}\text{C}_{\text{carb}}$  excursion and perturbation of global carbon cycle, termed the Lomagundi–Jatuli Event (LJE) between 2.22 Ga (or 2.31 Ga) and 2.06 Ga (Bekker & Holland, 2012; Karhu & Holland, 1996; Lajoinie et al., 2019; Martin, Condon, Prave, & Lepland, 2013; Martin, Condon, Prave, Melezhik, et al., 2013; Melezhik

et al., 2007; Melezhik & Fallick, 1996; Schidlowski et al., 1976). Records of the LJE are well preserved and carbonates with extremely high  $\delta^{13}\text{C}_{\text{carb}}$  values from 8‰ to >15‰ have been identified from many localities in North America, Russia, Finland, Africa, Australia, South America, Scotland, Norway, Sweden and India (Table 1). Although carbonates with  $\delta^{13}\text{C}_{\text{carb}}$  values of 5‰ were reported from the Guanmenshan Formation in the northeastern North China Craton (NCC) (Tang et al., 2008, 2011), no carbonate with  $\delta^{13}\text{C}_{\text{carb}}$  values of >6‰ has been identified, which resulted in highly controversial on existence of the LJE records in the NCC (Martin, Condon, Prave, & Lepland, 2013; Melezhik et al., 2013).

Recently, some researchers proposed that the  $\delta^{13}\text{C}_{\text{carb}}$  trend of LJE was linked to facies changes and argued that the LJE can be

neither construed as a priori as representative of the global carbon cycle or a planetary-scale disturbance to that cycle, nor as direct evidence for oxygenation of the ocean-atmosphere system (Bakakas Mayika et al., 2020; Prave et al., 2022). If valid, these new interpretations mean that the end of LJE was merely a facies shift from shallow-marine towards deeper-water settings (Bekker et al., 2021). Resolving whether the LJE was globally synchronous or asynchronous is essential for discriminating between different models (Hodgskiss et al., 2023). In this contribution, we present carbon-oxygen isotopes and chemical compositions of the newly confirmed ~2.20–2.06 Ga carbonates from Fanhe Basin in the northeastern NCC, and firstly identified carbonates with  $\delta^{13}\text{C}_{\text{carb}}$  values of 10.6‰–11.7‰ from the Daposhan Formation and 3.8‰–6.0‰ from the Kuangzhuangzi and Lower Tongjiajie formations. These new results provide solid evidence for existence of the LJE records in the NCC and global significance of the LJE.

## 2 | GEOLOGICAL SETTING, PREVIOUS STUDIES AND SAMPLES

The Fanhe Basin is located in the Longgang Block in the northeastern NCC (Figure 1a). Proterozoic successions in the basin were termed the Fanhe Group (or Sanchazi, Shuyatun and Huishitun groups) and are 8–9 km thick (Chen et al., 2006). They have an areal extent of 3300 km<sup>2</sup> and consist of marine carbonates, clastic rocks and minor mafic volcanic rocks that unconformably overlie Neoarchean basement rocks (Figure 1b). Proterozoic successions of the lower Fanhe Group have been divided into Daposhan, Kangzhuangzi, Guanmenshan and Tongjiajie formations from bottom to top, and were previously considered as Mesoproterozoic in age (Bureau of Geology and Mineral Resources of Liaoning Province (BGMRLP), 1989, 1997; Chen et al., 2006).

The Daposhan Formation consists of sandstone, sand-bearing dolostone and dolostone and components of carbonate increase from the bottom to top. The Kangzhuangzi Formation consists of sandstone, sand-bearing dolostone, phyllite and slate in its bottom, carbonaceous-rich slate and silty slate in the middle part, and micritic limestone and carbonaceous-rich limestone in its upper part. The Guanmenshan Formation consists of dolostone and minor sand-bearing dolostone. The Tongjiajie Formation consists of sand-bearing dolostone and sandstone in its lower part, and sandstone, silty dolostone and silty slate in its upper part. No evaporite has been identified. There is no sedimentary hiatus between the Daposhan, Kangzhuangzi, Guanmenshan and Tongjiajie formations, but a disconformity between the Tongjiajie Formation and the overlaying Hutouling Formation has been identified (Xu et al., 1997). Some carbonates were weakly recrystallized due to the emplacement of Proterozoic dolerite sills. Representative outcrop and photomicrographs are shown in Figures 2 and 3 and Figures S1–S6.

Previous researches show that carbonates from the Guanmenshan Formation have  $\delta^{13}\text{C}_{\text{V-PDB}}$  values of 3.5‰–5.9‰ and  $\delta^{18}\text{O}_{\text{V-SMOW}}$  values of 15.4‰–24.8‰ (Tang et al., 2008, 2011). However, the above positive excursion has neglected by many researchers studying GOE and LJE, mainly due to poor age constraints and low positive

## Significance Statement

The Lomagundi-Jatuli Event (LJE) represents Earth's largest known positive carbonate carbon isotope excursion and records of the LJE are well preserved in many cratons. However, no carbonate with high positive carbon isotope excursion has been identified in the North China Craton (NCC). Here we firstly identified marine carbonates with high positive  $\delta^{13}\text{C}_{\text{carb}}$  values of 10.6‰–11.7‰ from the Daposhan Formation in the newly confirmed Palaeoproterozoic successions in Fanhe Basin in the northeastern NCC. These new identified  $\delta^{13}\text{C}_{\text{carb}}$  values of 10.6‰–11.7‰ from the Daposhan Formation represent the largest positive carbonate carbon isotope excursion discovered in the NCC till present. The change of  $\delta^{13}\text{C}_{\text{carb}}$  values and end of the positive excursion in Fanhe Basin are unrelated to sedimentary facies and recrystallization, but are related to timing of deposition, which provide solid evidence for existence of the LJE records in North China as well as timing, magnitude and global significance of the positive  $\delta^{13}\text{C}_{\text{carb}}$  excursion of the LJE.

excursion when compared to the typical range in global  $\delta^{13}\text{C}_{\text{carb}}$  values of between -5‰ and 5‰ (Melezhik et al., 2013). Recent U-Pb geochronological results revealed that the Daposhan, Kangzhuangzi, Guanmenshan and Tongjiajie formations were deposited between ~2.20 Ga and 2.06 Ga (Cai et al., 2022). This new age is consistent with previous carbon-oxygen isotopes of carbonates from the Guanmenshan Formation (Tang et al., 2008, 2011), indicating deposition of the lower Fanhe Group as the same period as LJE. Different to other Palaeoproterozoic successions (Figure 1a) that were affected by 1.95–1.80 Ga high-grade metamorphism, the Palaeoproterozoic successions in Fanhe Basin are unmetamorphosed or low-grade metamorphosed (Figures 2 and 3). Therefore, the lower Fanhe Group represents the best-preserved geological records of GOE and LJE in the NCC (Cai et al., 2022). However, carbon-oxygen isotopes of carbonates from the Daposhan, Kangzhuangzi and Tongjiajie formations have not been analysed and it is not sure whether positive excursion exists.

Samples for carbon-oxygen isotopes and chemical compositions were mainly collected from the Daposhan, Kangzhuangzi, Guanmenshan and Tongjiajie formations in the lower Fanhe Group (Figures 1, 4 and 5). Some samples from the Hutouling and Shimen formations from the middle Fanhe Group were also collected for comparison. Lithology of samples is listed in Tables S1 and S2.

## 3 | ANALYTICAL METHODS

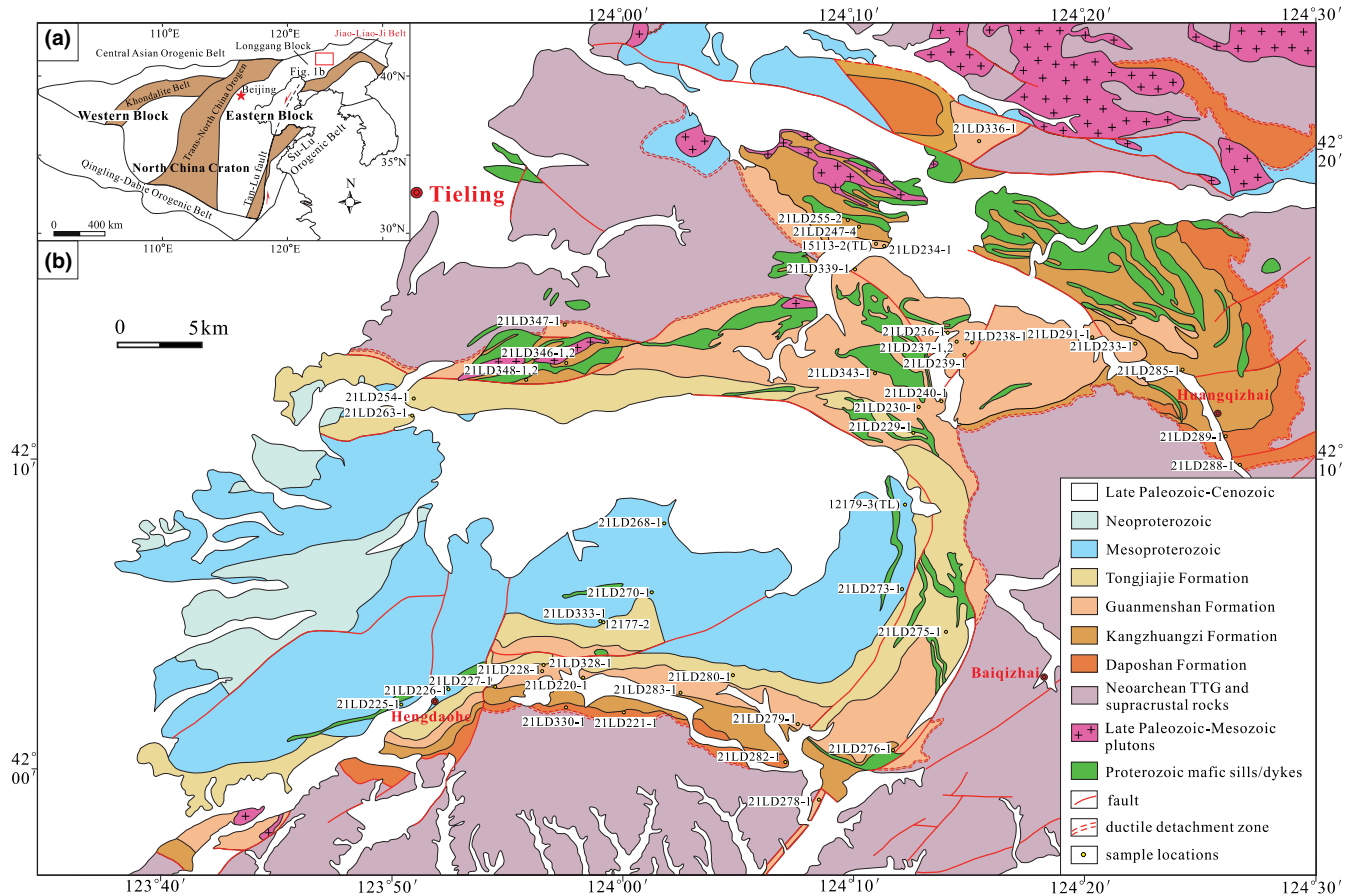
Carbon and oxygen isotope analyses were performed by using a Thermo Fisher Finnigan MAT-253 mass spectrometer at the Analytical Laboratory of the Beijing Research Institute of Uranium Geology

TABLE 1 Marine carbonates with  $\delta^{13}\text{C}_{\text{V}-\text{PDB}}$  values of +8‰ to >+15‰ as records of LJE (updated from Prave et al. (2022)).

Succession unit	Geographical or geological region	Country	Age (Ga)	$\delta^{13}\text{C}_{\text{V}-\text{PDB}}\text{ (‰)}$	References
Upper Duitschland Fm.	Transvaal Basin	South Africa	2.42–2.32	-2.2 to 10.2	Buick et al. (1998), Bekker et al. (2001), Frauenstein et al. (2009), Guo et al. (2009) and Schröder et al. (2016)
Silverton Fm.	Transvaal Basin	South Africa	2.20–2.10	6.8 to 11.1	Frauenstein et al. (2009), Guo et al. (2009) and Schröder et al. (2016)
Silverton Shale Fm.	Transvaal Basin	South Africa	2.20–2.10	3.8 to 10.7	Buick et al. (1998) and Schröder et al. (2016)
Lucknow Fm.	Transvaal Basin	South Africa	>2.2–2.1	1.8 to 11.4	Bekker et al. (2001), Frauenstein et al. (2009) and Schröder et al. (2008)
Lomagundi Group	Lomagundi Belt	Zimbabwe	>2.07	-4.9 to 13.4	Schildkamp et al. (1975)
Mcheka Fm.	Lomagundi Belt	Zimbabwe	>2.07	2.6 to 13.4	Schildkamp et al. (1976)
FB-FC	Francavillian succession	Gabon	2.19–2.08	-1.2 to 9.3	Bakakas Mayika et al. (2020) and Ossa Ossa et al. (2018)
FC-FD	Francavillian succession	Gabon	2.19–2.08	-2.5 to 9.7	Péret et al. (2011)
Buganda Group	Ruwenzori Mountains	Uganda	2.16–2.06	-9.3 to 11.3	Master et al. (2013)
Tulomozerskaya Fm. (drillholes)	Onega Basin	Russia	>2.1	5.6 to 17.2	Melezhik et al. (1999)
Tulomozero Fm.	Onega Basin	Russia	>2.1	5.8 to 15.5	Melezhik et al. (2015)
Tulomozero Fm.	South Karelian Subprovince	Russia	>2.1	6.0 to 11.5	Karhu (1993)
Jatulian Fm.	South Karelian Subprovince	Russia	>2.1	8.4 to 11.0	Karhu (1993)
Jatulian Fm.	Onega Basin	Russia	>2.1	10.6 to 15.9	Karhu (1993)
Kuetsjärvi Fm.	Pechenga Belt	Russia	~2.20–2.06	-1.0 to 8.9	Karhu (1993), Melezhik et al. (2003, 2005) and Salminen et al. (2013)
Loch Maree Group	Gairloch	Scotland	2.3–2.0	-5.1 to 15.4	Baker and Fallick (1989a) and Kerr et al. (2016)
Poikkijarvi Fm. (Hyrynsalmi Group)	Kalix Greenstone Belt	Sweden	>2.094	7.7 to 9.2	Karhu (1993)
Middle Group	Kalix Greenstone Belt	Sweden	<2.11	-0.3 to 8.5	Melezhik and Fallick (2010)
Middle Lapponian Group	Lapland and Kittilä-Kolari	Finland	>2.22–2.04	1.4 to 11.1	Karhu (1993)
Misi Dolomite	Peräpohja Schist Belt	Finland	2.22–2.12	11.6 to 13.0	Karhu (1993) and Niiranen et al. (2003)
Pyhäntunturi Fm.	Pelkosenniemi area	Finland	<2.13	5.3 to 12.6	Karhu (1993)
Sericite Schist Fm.	Kuusamo Schist Belt	Finland	2.30–2.206	8.1 to 8.2	Karhu (1993)
Dolomite Fm.	Kuusamo Schist Belt	Finland	>2.07	8.2 to 15.1	Karhu (1993)
Kvartsimaa Fm.	Peräpohja Schist Belt	Finland	2.44–2.10	8.3 to 9.2	Karhu (1993) and Köykkä et al. (2019)
Kivalo Fm.	Peräpohja Schist Belt	Finland	2.44–2.10	5.2 to 10.6	Karhu (1993) and Köykkä et al. (2019)
Rantamaa Fm.	North Ostrobothnia Schist Belt	Finland	>2.105	2.5 to 11.4	Karhu (1993) and Köykkä et al. (2019)
Kalevian succession	Gulf of Bothnia	Finland	>2.25–2.0	0.2 to 8.1	Karhu (1993)
Karelian Dolomite	Kainuu Schist Belt	Finland	>2.012	0 to 12.0	Schildkamp et al. (1975)
Upper Lapponian Group	Kainuu Schist Belt	Finland	>2.113	9.6 to 11.2	Karhu (1993)
Lower Viistola Fm.	Kiiltelysvaara	Finland	<2.113	<2.113	(Continues)

TABLE 1 (Continued)

Succession unit	Geographical or geological region	Country	Age (Ga)	$\delta^{13}\text{C}_{\text{VPDB}} (\text{\textperthousand})$	References
Lofoten-Vesterålen Jhamarkotra Fm.	Lofoten-Vesterålen Udaipur and neighbouring regions	Norway India	~2.1-2.0 2.15-2.07	-7.0 to 12.1 -5.4 to 11.9	Baker and Fallick (1989b) Purohit et al. (2010)
Slaughterhouse Fm.	Wyoming and South Dakota	USA	~2.15	5.9 to 16.6	Bekker et al. (2003)
Lower Nash Fork Fm.	Wyoming and South Dakota	USA	~2.15	0.1 to 28.2	Bekker et al. (2003)
Whalen Group	Wyoming and South Dakota	USA	~2.1-2.0	-0.3 to 8.2	Bekker et al. (2003)
Lower Albanel Fm.	Lakes Mistassini and Albanel, Québec and Labrador Trough, Québec and Labrador	Canada Canada	2.13-2.07 ~2.169	-6.1 to 8.2 14.2 to 15.4	Mirota and Veizer (1994) and Schidlowski et al. (1983) Melezlik et al. (1997)
Dunphy Fm.	Alder Fm.	Canada	2.169-2.142	8.7 to 10.2	Melezlik et al. (1997)
Uvée Fm.	Labrador Trough, Québec and Labrador	Canada	2.169-2.142	5.3 to 10.4	Melezlik et al. (1997)
Waterson Fm.	Quartzite Lake area	Canada	>2.10 or <1.91(?)	8.3 to 8.5	Aspler et al. (2002) and Hofmann and Davidson (1998)
Gordon Lake Fm.	Lake Superior area	USA, Canada	~2.45-2.22	-1.0 to 8.2	Bekker et al. (2006)
Konai Dolomite	Lake Superior area	USA, Canada	~2.3-2.22	1.9 to 9.5	Bekker et al. (2006)
Alto Moxotó Terrane (Itatuba Marble)	Borborema	Brazil	2.25-1.91	-3.3 to 8.8	Santos et al. (2013)
Woolly Dolomite	Capricorn Orogen	Australia	~2.03	-7.1 to 8.4	Bekker et al. (2016)
Meta-carbonate rocks (Kongling Complex)	Yangtze Craton, South China	China	~2.0	5.5 to 11.6	Li et al. (2022)
	Fanhe Basin, North China Craton	China	~2.2-2.1	10.2 to 11.8	This study
	Daposhan Fm.				



**FIGURE 1** Geological map of the Fanhe Basin and sample locations (modified after Cai et al. (2022) and Chen et al. (2006). [Colour figure can be viewed at [wileyonlinelibrary.com](http://wileyonlinelibrary.com)]

and the State Key Laboratory of Geological Processes and Mineral Resources of China University of Geosciences, Wuhan following methods described by Shen et al. (2012), Yang et al. (2013) and Li, Li, et al., 2020. Whole-rock major element analyses were performed using a Rigaku ZSX Primus II X-ray fluorescence at the Wuhan Sample Solution Analytical Technology Company Limited. Detailed operating conditions for laboratory procedures and data reduction are listed in Data S1.

## 4 | RESULTS

### 4.1 | Carbon–oxygen isotopes of carbonate rocks

Carbon–oxygen isotopes are listed in Table S1 and plotted in Figures 4 and 5. The Daposhan Formation has strongly positive  $\delta^{13}\text{C}_{\text{V-PDB}}$  values of 11.8‰–10.2‰ and  $\delta^{18}\text{O}_{\text{V-SMOW}}$  values of 22.0‰–19.2‰. The Kangzhuangzi Formation has positive  $\delta^{13}\text{C}_{\text{V-PDB}}$  values of 6.0‰–3.8‰ and  $\delta^{18}\text{O}_{\text{V-SMOW}}$  values of 20.2‰–15.2‰. The Guanmenshan Formation has positive  $\delta^{13}\text{C}_{\text{V-PDB}}$  values of 6.8‰–3.9‰ and  $\delta^{18}\text{O}_{\text{V-SMOW}}$  values of 25.4‰–14.9‰. The Lower Tongjiajie Formation has positive  $\delta^{13}\text{C}_{\text{V-PDB}}$  values of 4.7‰–4.3‰ and  $\delta^{18}\text{O}_{\text{V-SMOW}}$  values of 20.8‰–20.7‰. The Upper Tongjiajie Formation has  $\delta^{13}\text{C}_{\text{V-PDB}}$  values from 2.0‰ to −0.7‰ and  $\delta^{18}\text{O}_{\text{V-SMOW}}$  values of 22.3‰–12.0‰. The Hutouling Formation has  $\delta^{13}\text{C}_{\text{V-PDB}}$

values from 1.0‰ to −0.2‰ and  $\delta^{18}\text{O}_{\text{V-SMOW}}$  values of 23.7‰–15.9‰. The Shimen Formation has  $\delta^{13}\text{C}_{\text{V-PDB}}$  values of 1.5‰ and  $\delta^{18}\text{O}_{\text{V-SMOW}}$  values of 22.5‰–22.4‰.

### 4.2 | Major element compositions

Major element compositions are listed in Table S2. They are characterized by large variable  $\text{SiO}_2$  contents from 0.12 wt.% to 52.97 wt.% and  $\text{Al}_2\text{O}_3$  contents of 0–5.35 wt.%. Their  $\text{CaO}$  contents range from 15.51 wt.% to 53.88 wt.% and  $\text{MgO}$  contents range from 0.38 wt.% to 22.46 wt.%. The carbon–oxygen isotopic compositions show no correlation with contents of  $\text{SiO}_2$ ,  $\text{Ti}$ ,  $\text{Al}_2\text{O}_3$ ,  $\text{Fe}_{2}\text{O}_3$ ,  $\text{Mn}$ ,  $\text{Na}_2\text{O}$ ,  $\text{K}_2\text{O}$ ,  $\text{P}_2\text{O}_5$  and  $\text{Ca}/\text{Mg}$  ratios (Figures 4 and 5).

## 5 | DISCUSSION

### 5.1 | Positive $\delta^{13}\text{C}_{\text{carb}}$ excursion identified in the lower Fanhe Group

Our new results show that all marine carbonates from the Lower Tongjiajie, Guanmenshan, Kangzhuangzi and Daposhan formations are characterized by positive carbon isotope excursion with  $\delta^{13}\text{C}_{\text{carb}}$

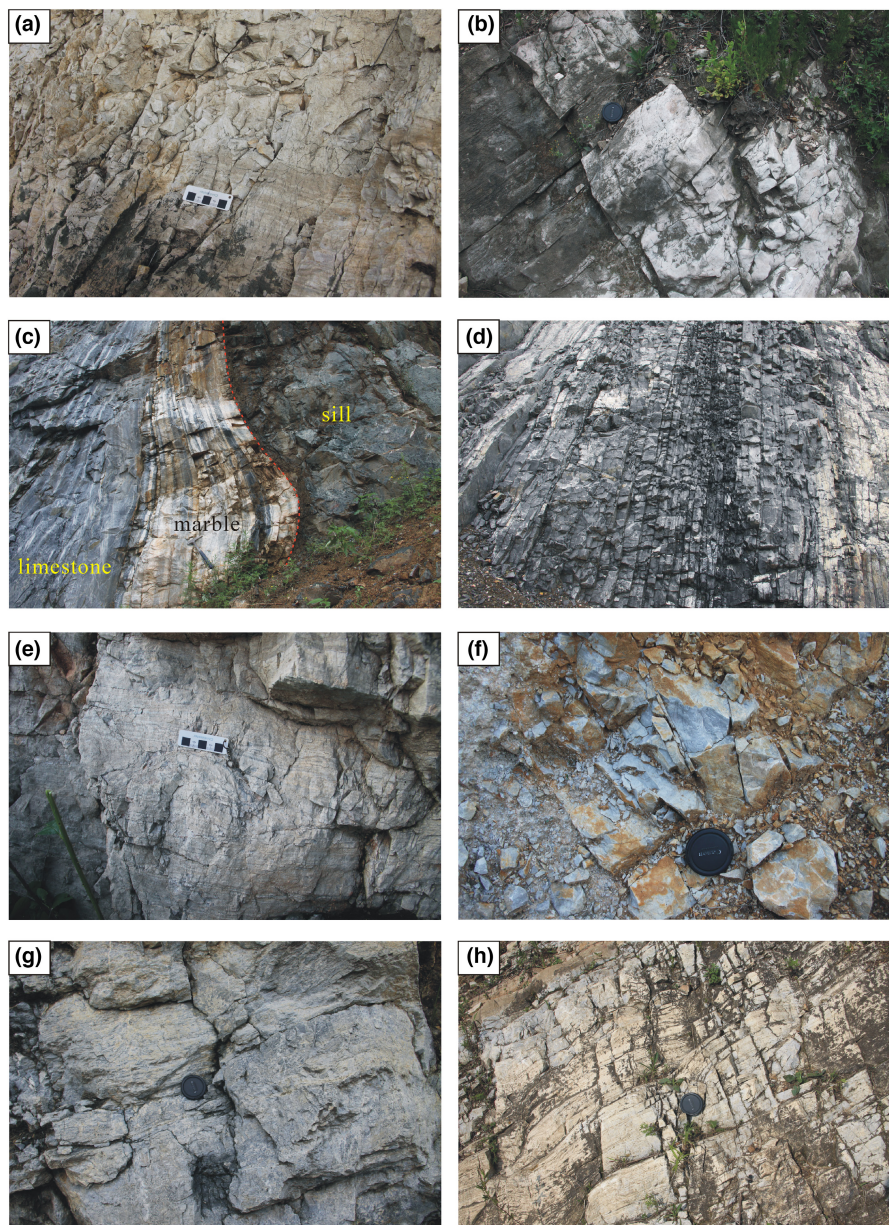


**FIGURE 2** Representative outcrop photographs of the lower part of the Fanhe Group. (a) Sand-bearing dolostone in southern Fanhe Basin (Daposhan Formation, site 21LD330, GPS position: 123°57.6' E; 42°02.0' N). (b) Sand-bearing dolomitic marble in southern Fanhe Basin (Daposhan Formation, site 21LD221, GPS position: 124°00.1' E; 42°02.0' N). (c) Limestone and recrystallized limestone related to contact metamorphism during emplacement of Proterozoic dolerite sills in northeastern Fanhe Basin (Kangzhuangzi Formation, site 21LD248, GPS position: 124°10.0' E; 42°17.6' N). (d) Limestone and carbonaceous-rich slate in northwestern Fanhe Basin (Kangzhuangzi Formation, site 21LD246, GPS position: 124°09.5' E; 42°18.1' N). (e) Dolostone in southern Fanhe Basin (Guanmenshan Formation, site 21LD227, GPS position: 123°54.4' E; 42°02.6' N). (f) Dolomitic marble in southern Fanhe Basin (Guanmenshan Formation, site 21LD228, GPS position: 123°56.5' E; 42°03.1' N). (g) Argillaceous dolostone from the Lower Tongjiajie Formation in southern Fanhe Basin (site 21LD275, GPS position: 124°14.1' E; 42°04.4' N). (h) Sand-bearing dolostone from the Upper Tongjiajie Formation in southern Fanhe Basin (site 21LD280, GPS position: 124°04.8' E; 42°02.9' N). [Colour figure can be viewed at [wileyonlinelibrary.com](http://wileyonlinelibrary.com)]

values mostly >5‰, consisting with their deposition ages of ~2.20–2.06 Ga (Cai et al., 2022). Specially, those from the Daposhan Formation have high positive  $\delta^{13}\text{C}_{\text{carb}}$  values of 10.2‰–11.8‰, which is the largest positive  $\delta^{13}\text{C}_{\text{carb}}$  excursion identified in the NCC. In contrast, carbonates from the Upper Tongjiajie, Hutouling and Shimen formations exhibit normal  $\delta^{13}\text{C}_{\text{carb}}$  compositions, consisting with their deposition after 2.06 Ga (Cai et al., 2022).

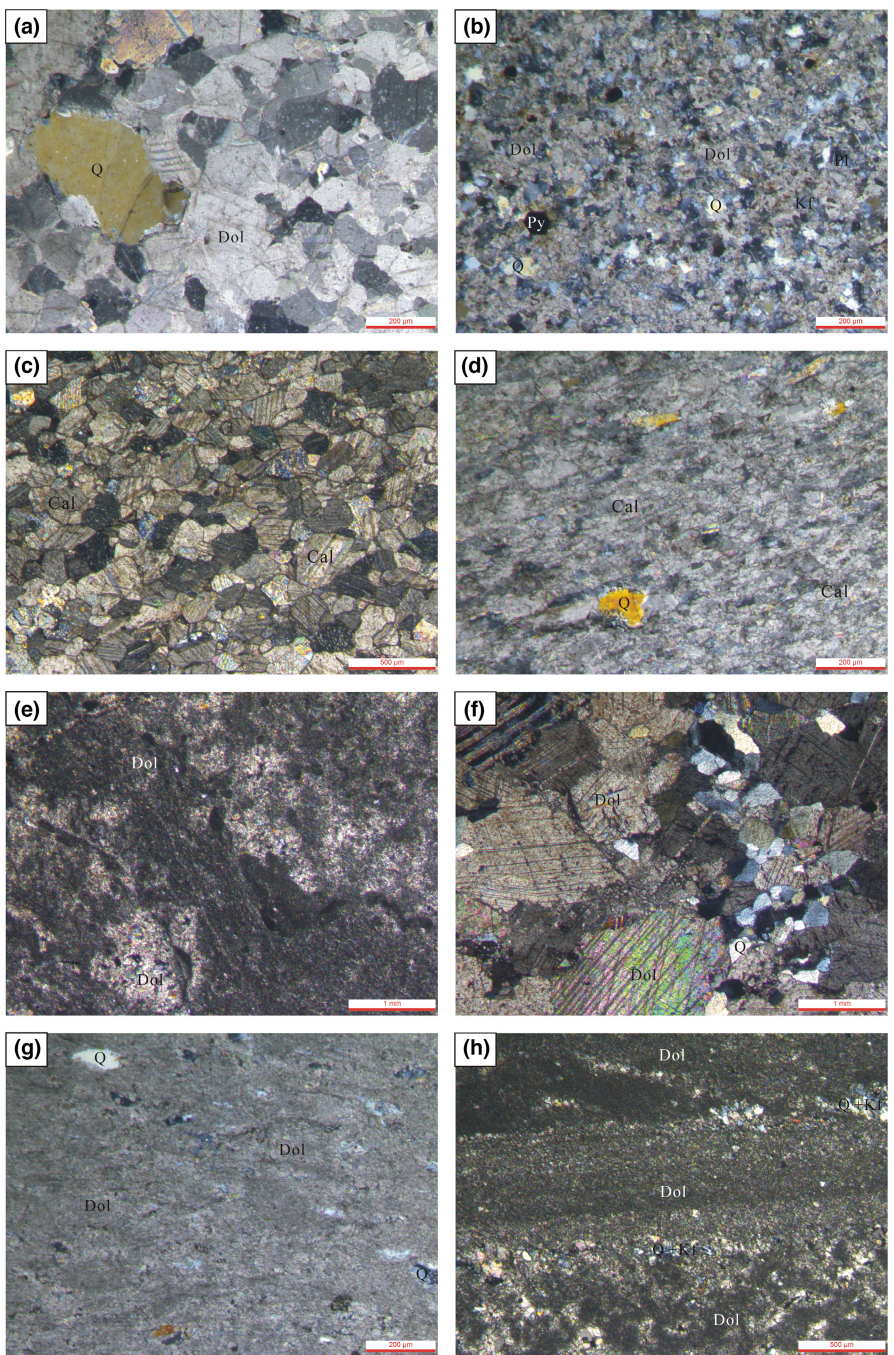
On  $\delta^{18}\text{O}_{\text{carb}}$  versus  $\delta^{13}\text{C}_{\text{carb}}$  plot (Figure 6), there is no correlation between  $\delta^{18}\text{O}_{\text{carb}}$  and  $\delta^{13}\text{C}_{\text{carb}}$  values and most samples have  $\delta^{18}\text{O}_{\text{V-SMOW}}$  values >18‰, indicating that their carbon–oxygen isotopic compositions were not significantly affected by late geological processes and represent those of the original sedimentary carbonate protolith. Some dolomitic marbles and recrystallized limestones have low  $\delta^{18}\text{O}_{\text{V-SMOW}}$  values <16.0‰ ( $\delta^{18}\text{O}_{\text{V-PDB}}$  values <-14.5‰) due to recrystallization, but their  $\delta^{13}\text{C}_{\text{carb}}$  values remain unaffected. Our carbon–oxygen isotopes confirm existence of positive  $\delta^{13}\text{C}_{\text{carb}}$  excursion of ~5‰ in the Guanmenshan

Formation as previously suggested (Tang et al., 2008, 2011), and identified positive  $\delta^{13}\text{C}_{\text{carb}}$  excursions of ~5‰ from the Lower Tongjiajie and Kangzhuangzi formations and of 10.2‰–11.8‰ from the Daposhan Formation in the lower Fanhe Group. The Palaeoproterozoic carbonates with positive  $\delta^{13}\text{C}_{\text{carb}}$  values we reported in the Fanhe Basin are ~3–4 km thick with an areal extent of 3300 km<sup>2</sup>, and represent the best-preserved geological records for the LJE in China.

## 5.2 | Comparing C–O isotopes of carbonates with different lithology, sedimentary facies and chemical compositions

Lithology of the lower Fanhe Group shows that deposition of the Daposhan Formation occurred in supralittoral tidal and intertidal zones; the Kangzhuangzi Formation occurred in intertidal to

**FIGURE 3** Representative photomicrographs (cross polarized light) of the lower part of the Fanhe Group. (a) Dolomitic marble (Daposhan Formation, sample 21LD288-1, GPS position: 124°26.5' E; 42°09.9' N). (b) Sand-bearing dolostone (Daposhan Formation, sample 21LD330-1, GPS position: 123°57.6' E; 42°02.0' N). (c) Recrystallized limestone near the contact between lime stone and Proterozoic dolerite sill (Kangzhuangzi Formation, sample 21LD348-1, GPS position: 123°55.7' E; 42°12.6' N). (d) Limestone (Kangzhuangzi Formation, sample 21LD348-2, GPS position: 123°55.7' E; 42°12.6' N). (e) Dolostone in southern Fanhe Basin (Guanmenshan Formation, sample 21LD220-1, GPS position: 123°58.2' E; 42°02.9' N). (f) Sand-bearing dolomitic marble in northwestern Fanhe Basin (Guanmenshan Formation, sample 21LD347-1, GPS position: 123°57.5' E; 42°14.5' N). (g) Argillaceous dolostone from the Lower Tongjiajie Formation in southern Fanhe Basin (21LD275-1, GPS position: 124°14.1' E; 42°04.4' N). (h) Sand-bearing dolostone from the Upper Tongjiajie Formation in southern Fanhe Basin (21LD280-1, GPS position: 124°04.8' E; 42°02.9' N). Mineral abbreviations: Dol, dolomite; Cal, calcite; Q, quartz; Pl, plagioclase; Kf, K-feldspar; Py, pyrite. [Colour figure can be viewed at [wileyonlinelibrary.com](http://wileyonlinelibrary.com)]



infralittoral zone and shallow-marine shelf; the Guanmenshan Formation occurred in shallow-marine reef; and the Tongjiajie Formation occurred in shallow-marine reef and offshore beach (Figures 4 and 5, Xu et al., 1997; Chen et al., 2006). The water depths increase from the Daposhan to Kangzhuangzi formations and reach the highest sea level in the upper Kangzhuangzi Formation, and then decrease from Guanmenshan to Tongjiajie formations (Figures 4 and 5). The large variable SiO<sub>2</sub> (0.12–52.97 wt.%), Al<sub>2</sub>O<sub>3</sub> (0–5.35 wt.%) and TiO<sub>2</sub> contents (0.002–0.294 wt.%) indicate differential involvement of terrigenous clastics or clays. Since some recent results considered the  $\delta^{13}\text{C}_{\text{carb}}$  trend of the LJE as facies dependent and challenged the global meaning of the LJE (Bakakas Mayika et al., 2020; Prave

et al., 2022), whether the positive  $\delta^{13}\text{C}_{\text{carb}}$  excursions in the lower Fanhe Group is related to lithology and facies changes should be examined.

Comparing carbon-oxygen isotopes of carbonate rocks with different lithology and chemical compositions shows that there is no correlation between  $\delta^{13}\text{C}_{\text{carb}}$  values and lithology, SiO<sub>2</sub>, Ti, Al<sub>2</sub>O<sub>3</sub>, TFe<sub>2</sub>O<sub>3</sub>, Mn, Na<sub>2</sub>O, K<sub>2</sub>O and P<sub>2</sub>O<sub>5</sub> contents and Ca/Mg ratios (Figures 4 and 5), indicating that the  $\delta^{13}\text{C}_{\text{carb}}$  values are unrelated to lithology and chemical compositions. During deposition of the Tongjiajie Formation, sedimentary facies changed from shallow-marine reef setting in its lower part ( $\delta^{13}\text{C}_{\text{carb}}$  values of ~5‰) to offshore beach setting in its upper part ( $\delta^{13}\text{C}_{\text{carb}}$  values

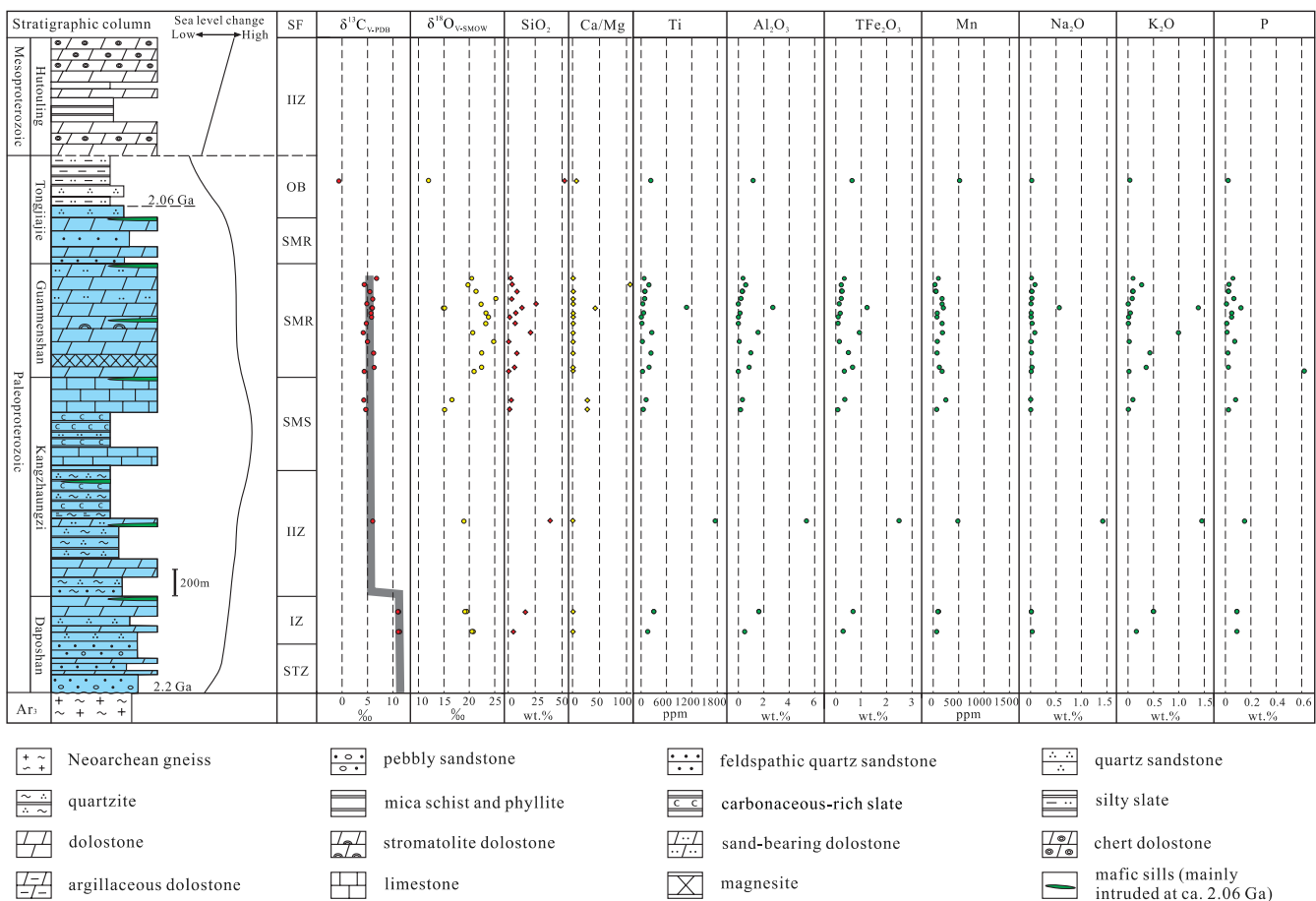


**FIGURE 4** Lithostratigraphic columns, C-O isotopes and major element compositions of the lower and middle parts of the Fanhe Group in the northeastern Fanhe Basin. [Colour figure can be viewed at [wileyonlinelibrary.com](http://wileyonlinelibrary.com)]

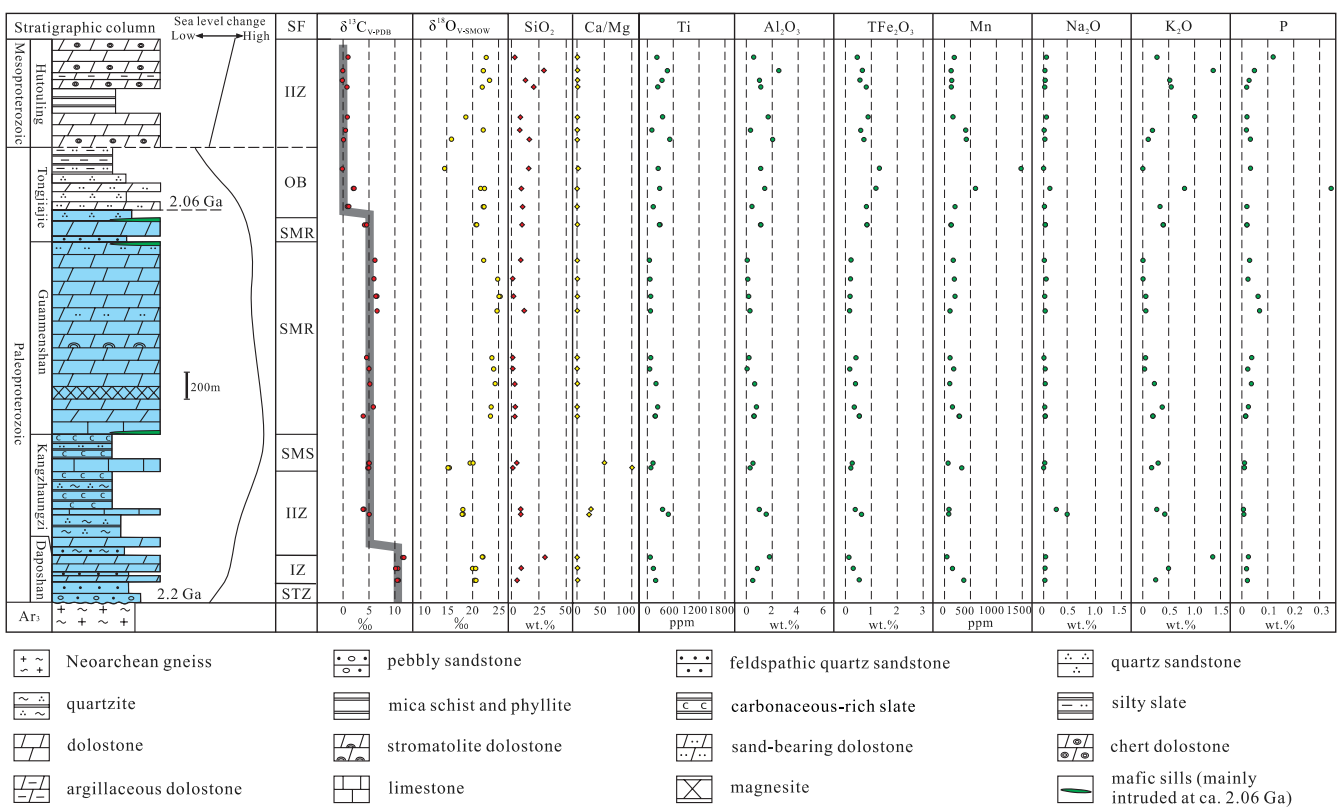
of  $\sim 0\text{\textperthousand}$ ), which is inconsistent with the previous inferences that shallow-marine setting is marked by the strongly positive values, whereas deeper-marine setting is characterized by weak or no positive excursions (Bakakas Mayika et al., 2020; Prave et al., 2022). Moreover, there is no difference between  $\delta^{13}\text{C}_{\text{carb}}$  values of the recrystallized and unrecrystallized carbonates (Figure 6). In fact, samples from the same formations in different locations have similar  $\delta^{13}\text{C}_{\text{carb}}$  values (Figures 4 and 5), indicating that the positive carbon isotope excursion we identified is facies independent and represents a strong perturbation of the global carbon cycle recorded in the NCC.

### 5.3 | Implications for global record of GOE and LJE

Although Chen (1988) firstly proposed a palaeoenvironmental catastrophe at  $\sim 2.3\text{ Ga}$  by studying the REE geochemistry of the Palaeoproterozoic high-grade metamorphosed sediments in the southern NCC (Chen, 1990; Chen & Zhao, 1997), intensive metamorphism, poor age constraints and lack of reliable diamictites and carbonates with strong positive carbon isotope excursion in the

Palaeoproterozoic successions seriously restricted the studying of GOE and LJE in the NCC (Melezhik et al., 2013).

Our results show that all marine carbonates from the Daposhan, Kangzhuangzi, Guanmenshan and Lower Tongjajie formations are characterized by positive  $\delta^{13}\text{C}_{\text{carb}}$  values from  $\sim 5\text{\textperthousand}$  to  $\sim 11\text{\textperthousand}$  and represent the largest positive  $\delta^{13}\text{C}_{\text{carb}}$  excursion identified in the NCC, and those from the Upper Tongjajie Formation and the overlying Hutouling and Shimen formations have no positive carbon isotope excursion. There is no correlation between  $\delta^{13}\text{C}_{\text{carb}}$  values and their chemical compositions, indicating that the positive carbon isotope excursion is facies independent. Deposition of the marine carbonates with positive carbon isotope excursion occurred during  $\sim 2.2\text{--}2.06\text{ Ga}$  and carbonates with no carbon isotope excursion were deposited after 2.06 Ga. The above deposition ages and carbon isotope in Fanhe Basin are consistent with timing of the LJE occurred mostly between 2.22 Ga and 2.06 Ga and termination of the LJE at 2.06 Ga constrained in other continents (Bekker & Holland, 2012; Karhu & Holland, 1996; Lajoinie et al., 2019; Melezhik & Fallick, 1996; Table 1). In the deposition age versus  $\delta^{13}\text{C}_{\text{V-PDB}}$  plot (Figure 7), the  $\delta^{13}\text{C}_{\text{V-PDB}}$  values of carbonates from the lower Fanhe Group are similar to those of carbonates from other cratons and



Sedimentary facies (SF): supralittoral tidal zone (STZ); intertidal zone (IZ); intertidal to infralittoral zone (IIZ); shallow-marine shelf (SMS); shallow-marine reef (SMR); offshore beach (OB)

FIGURE 5 Lithostratigraphic columns, C-O isotopes and major element compositions of the lower and middle parts of the Fanhe Group in the southern Fanhe Basin. [Colour figure can be viewed at [wileyonlinelibrary.com](http://wileyonlinelibrary.com)]

FIGURE 6  $\delta^{18}\text{O}_{\text{V-SMOW}}$  versus  $\delta^{13}\text{C}_{\text{V-PDB}}$  plot for carbonate rocks from the lower and middle parts of the Fanhe Group. [Colour figure can be viewed at [wileyonlinelibrary.com](http://wileyonlinelibrary.com)]

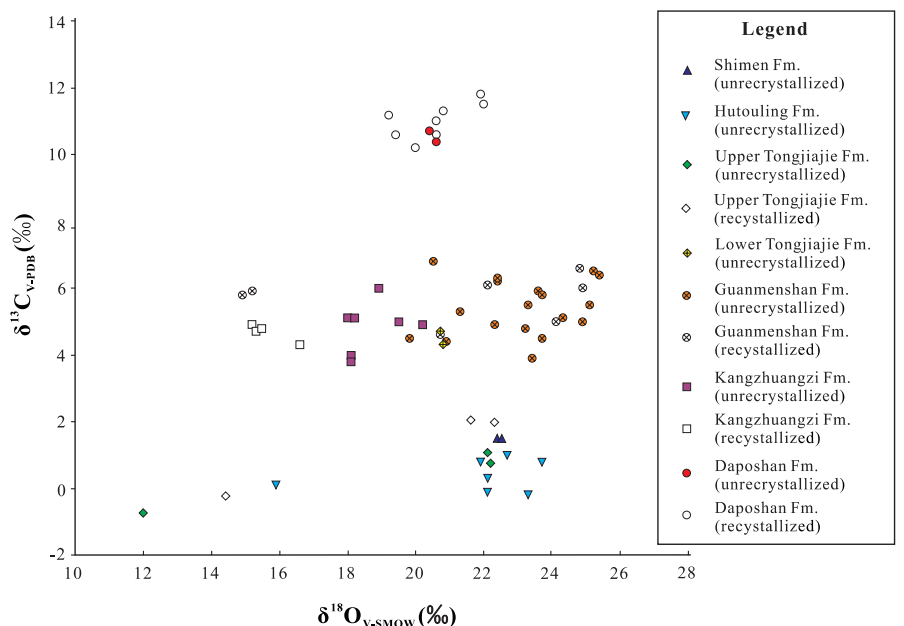
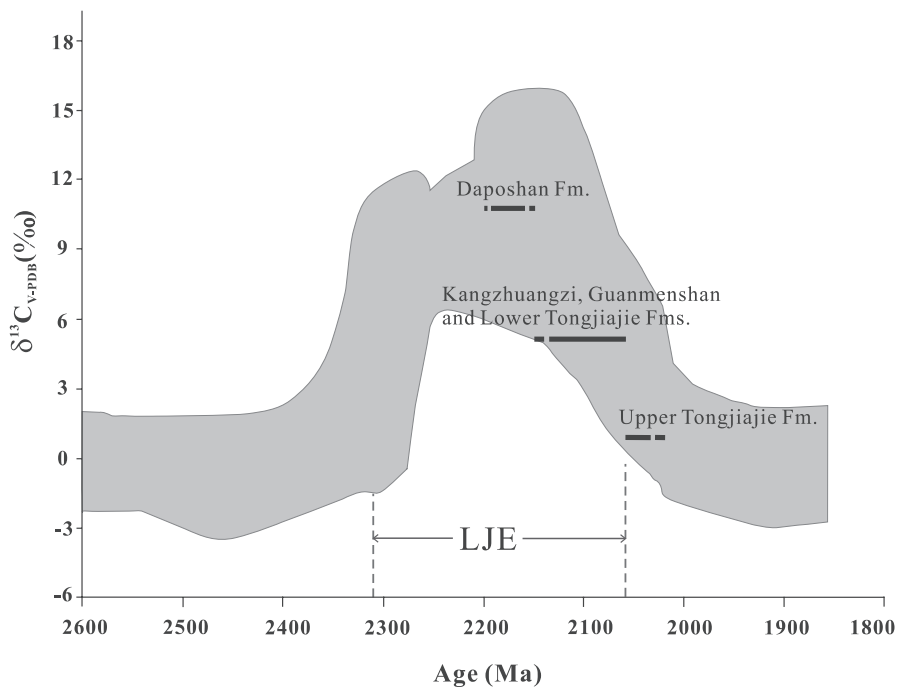


exhibit a decreasing trend from ~2.2 Ga to 2.06 Ga as other cratons. Similar deposition ages and variation trend from 2.22 Ga to 2.06 Ga between the carbonates with positive carbon isotope excursion newly identified in the NCC and those in other continents (Table 1)

confirm that the LJE is a globally synchronous event and represent the largest perturbation of the global carbon cycle in Earth's history (Martin, Condon, Prave, & Lepland, 2013; Melezhik et al., 2007; Melezhik et al., 2013).



**FIGURE 7** Deposition age versus  $\delta^{13}\text{C}_{\text{V}-\text{PDB}}$  plot for marine carbonates (shaded area) from the Palaeoproterozoic successions (modified after Melezhik et al. (2013) and Prave et al. (2022)). The  $\delta^{13}\text{C}_{\text{V}-\text{PDB}}$  values of marine carbonates from the lower Fanhe Group are shown for comparison.

## 6 | CONCLUSIONS

Our results show that the ~2.20–2.06 Ga carbonates from the newly confirmed Palaeoproterozoic successions in the lower Fanhe Group in the northeastern NCC have high positive carbon isotope excursion similar to the carbonates deposited during LJE in other continents. We firstly identified marine carbonates with  $\delta^{13}\text{C}_{\text{carb}}$  values of 10.6‰–11.7‰ from the Daposhan Formation and of 3.8‰–6.0‰ from the Kuangzhuangzi and Lower Tongjajie formations. The carbonates of the Daposhan Formation record the largest positive carbon isotope excursion identified in the NCC.

The ~2.20–2.06 Ga marine carbonates in Fanhe Basin have similar  $\delta^{13}\text{C}_{\text{carb}}$  values as those synchronously deposited in other cratons and their  $\delta^{13}\text{C}_{\text{carb}}$  values exhibit a decreasing trend from ~2.20 Ga to 2.06 Ga. These ~3–4 km thick Palaeoproterozoic carbonates with positive  $\delta^{13}\text{C}_{\text{carb}}$  values represent the best-preserved geological records for LJE in China. Our identification of carbonates with high positive carbon isotope excursion shed new lights on the geological records of the LJE in the NCC as well as timing, magnitude and global significance of the positive  $\delta^{13}\text{C}_{\text{carb}}$  excursion of LJE.

## ACKNOWLEDGMENTS

This research was financially supported by the National Natural Science Foundation of China (41920104004, 41725011, U2244213). We thank Jun Shen for help during C-O isotopic analyses.

## DATA AVAILABILITY STATEMENT

The data that supports the findings of this study are available in the supplementary material of this article.

## REFERENCES

- Aspler, L. B., Cousens, B. L., & Chiarenzelli, J. G. (2002). Griffin gabbro sills (2.11 Ga), Hurwitz Basin, Nunavut, Canada: Long-distance lateral transport of magmas in western Churchill Province crust. *Precambrian Research*, 117, 269–294.
- Bakakas Mayika, K., Moussavou, M., Prave, A. R., Lepland, A., Mbina, M., & Kirsimäe, K. (2020). Paleoproterozoic Francevillian succession of Gabon and the Lomagundi-Jatuli event. *Geology*, 48, 1099–1104.
- Baker, A. J., & Fallick, A. E. (1989a). Evidence from Lewisian limestones for isotopically heavy carbon in two thousand million year old seawater. *Nature*, 337, 352–354.
- Baker, A. J., & Fallick, A. E. (1989b). Heavy carbon in two-billion-year-old marbles from Lofoten-Vesterålen, Norway: Implications for the Precambrian carbon cycle. *Geochimica et Cosmochimica Acta*, 53, 1111–1115.
- Bekker, A., El Albani, A., Hofmann, A., Karhu, J. A., Kump, L., Ossa Ossa, F., & Planavsky, N. (2021). The Paleoproterozoic Francevillian succession of Gabon and the Lomagundi-Jatuli event: Comment. *Geology*, 49, e527.
- Bekker, A., & Holland, H. D. (2012). Oxygen overshoot and recovery during the early Paleoproterozoic. *Earth and Planetary Science Letters*, 317, 295–304.
- Bekker, A., Holland, H. D., Wang, P. L., Rumble, D., Stein, H. J., Hannah, J. L., Coetze, L. L., & Beukes, N. J. (2004). Dating the rise of atmospheric oxygen. *Nature*, 427, 117–120.
- Bekker, A., Karhu, J. A., Eriksson, K. A., & Kaufman, A. J. (2003). Chemostratigraphy of Paleoproterozoic carbonate successions of the Wyoming Craton: Tectonic forcing of biogeochemical change? *Precambrian Research*, 120, 279–325.
- Bekker, A., Karhu, J. A., & Kaufman, A. J. (2006). Carbon isotope record for the onset of the Lomagundi carbon isotope excursion in the Great Lakes area, North America. *Precambrian Research*, 148, 145–180.
- Bekker, A., Kaufman, A. J., Karhu, J. A., Beukes, N. J., Swart, Q. D., Coetze, L. L., & Eriksson, K. A. (2001). Chemostratigraphy of the Paleoproterozoic Duitschland Formation, South Africa: Implications for coupled climate change and carbon cycling. *American Journal of Science*, 301, 261–285.

- Bekker, A., Krapež, B., Müller, S. G., & Karhu, J. A. (2016). A short-term, post-Lomagundi positive C isotope excursion at c. 2.03 Ga recorded by the Wooly Dolomite, Western Australia. *Journal of the Geological Society*, 173, 689–700.
- Buick, I. S., Uken, R., Gibson, R. L., & Wallmach, T. (1998). High- $\delta^{13}\text{C}$  Paleoproterozoic carbonates from the Transvaal Supergroup, South Africa. *Geology*, 26, 875–878.
- Bureau of Geology and Mineral Resources of Liaoning Province (BGMRLP). (1989). *Regional geology of Liaoning Province* (p. 858). Geological Memoirs, ser. 1, no. 14, (in Chinese with English abstract). Geological Publishing House.
- Bureau of Geology and Mineral Resources of Liaoning Province (BGMRLP). (1997). *Stratigraphy (Lithostratic) of Liaoning Province: Multiple classification and correlation of the stratigraphy of China No. 21* (p. 247). China University of Geosciences Press (in Chinese).
- Cai, Y., Zhang, S., Zhao, Y., Hu, G., Zhang, Q., & Pei, J. (2022). Ages of the Proterozoic strata in Fanhe Basin revisited: Implications for geological records of the Great Oxidation Event in the North China Craton. *Precambrian Research*, 368, 106466.
- Canfield, D. E. (2005). The early history of atmospheric oxygen: Homage to Robert M. Garrels. *Annual Review of Earth and Planetary Sciences*, 33, 1–36.
- Chen, S. W., Xing, D. H., & Ding, Q. H. (2006). 1:250,000 geological map and explanatory note of Tieling, K51C00200. Shenyang Institute of Geology and Mineral Resources. <https://doi.org/10.35080/n01.c.123080> (in Chinese).
- Chen, Y. J. (1988). Catastrophe of the geological environment at 2300 Ma (pp. 11). In: Abstracts of the Symposium on Geochemistry and Mineralization of Proterozoic Mobile Belts, September 6–10, 1988, Tianjin, China.
- Chen, Y. J. (1990). Evidences for the catastrophe in geologic environment at about 2300 Ma and the discussions on several problems. *Journal of Stratigraphy*, 14(3), 178–184. (in Chinese with English abstract).
- Chen, Y. J., & Zhao, Y. C. (1997). Geochemical characteristics and evolution of REE in the early Precambrian sediments: Evidences from the southern margin of the North China craton. *Episodes*, 20(2), 109–116.
- Frauenstein, F., Veizer, J., Beukes, N., Van Niekerk, H. S., & Coetze, L. L. (2009). Transvaal Supergroup carbonates: Implications for Paleoproterozoic  $\delta^{18}\text{O}$  and  $\delta^{13}\text{C}$  records. *Precambrian Research*, 175, 149–160.
- Gumsley, A. P., Chamberlain, K. R., Bleeker, W., Soderlund, U., de Kock, M. O., Larsson, E. R., & Bekker, A. (2017). The timing and tempo of the Great Oxidation Event. *Proceedings of the National Academy of Sciences of the United States of America*, 114, 18111–1816.
- Guo, Q., Strauss, H., Kaufman, A. J., Schröder, S., Gutzmer, J., Wing, B., Baker, M. A., Bekker, A., Jin, Q., Kim, S.-T., & Farquhar, J. (2009). Reconstructing Earth's surface oxidation across the Archean-Proterozoic transition. *Geology*, 37, 399–402.
- Hodgskiss, M. S. W., Crockford, P. W., & Turchyn, A. V. (2023). Deconstructing the Lomagundi-Jatuli carbon isotope excursion. *Annual Review of Earth and Planetary Sciences*, 51, 301–330.
- Hofmann, H. J., & Davidson, A. (1998). Paleoproterozoic stromatolites, Hurwitz Group, Quartzite Lake area, Northwest Territories, Canada. *Canadian Journal of Earth Sciences*, 35, 280–289.
- Holland, H. D. (1999). When did the Earth's atmosphere become oxic? A reply. *The Geochemical News*, 100, 21–23.
- Holland, H. D. (2002). Volcanic gases, black smokers, and the Great Oxidation Event. *Geochimica et Cosmochimica Acta*, 66, 3811–3826.
- Holland, H. D. (2009). Why the atmosphere became oxygenated: A proposal. *Geochimica et Cosmochimica Acta*, 73, 5241–5255.
- Karhu, J. A. (1993). Paleoproterozoic evolution of the carbon isotope ratios of sedimentary carbonates in the Fennoscandian shield. *Geological Survey of Finland Bulletin*, 371, 1–87.
- Karhu, J. A., & Holland, H. D. (1996). Carbon isotopes and the rise of atmospheric oxygen. *Geology*, 24, 867–870.
- Kerr, G. B., Prave, A. R., Martin, A. P., Fallick, A. E., Brasier, A. T., & Park, R. G. (2016). The Palaeoproterozoic global carbon cycle: Insights from the Loch Maree Group, NW Scotland. *Journal of the Geological Society*, 173, 170–176.
- Konhauser, K. O., Pecoits, E., Lalonde, S. V., Papineau, D., Nisbet, E. G., Barley, M. E., Arndt, N. T., Zahnle, K., & Kamber, B. S. (2009). Oceanic nickel depletion and a methanogen famine before the Great Oxidation Event. *Nature*, 458, 750–753.
- Köykkä, J., Lahtinen, R., & Huhma, H. (2019). Provenance evolution of the Paleoproterozoic metasedimentary cover sequences in northern Fennoscandia: Age distribution, geochemistry, and zircon morphology. *Precambrian Research*, 331, 105364.
- Kump, L. R. (2008). The rise of atmospheric oxygen. *Nature*, 451, 277–278.
- Lajoinie, M. F., Sial, A., Justiniano, C. A. B., Cingolani, C. A., Recio, C., Etchegorry, R. O., Basei, M., & Lanfranchini, M. E. (2019). First geochronological constraint for the Palaeoproterozoic Lomagundi-Jatuli  $\delta^{13}\text{C}$  anomaly in the Tandilia Belt basement (Argentina), Rio de la Plata Craton. *Precambrian Research*, 334, 105477.
- Li, Q., Li, L., Zhang, Y., & Guo, Z. (2020). Oligocene incursion of the Paratethys seawater to the Junggar Basin, NW China: Insight from multiple isotopic analysis of carbonate. *Scientific Reports*, 10, 6601.
- Li, Y., Satish-Kumar, M., Kiran, S., Wan, C., & Zheng, J. (2022). 2.0 Ga orogenic graphite deposits and associated  $^{13}\text{C}$ -enriched meta-carbonate rocks from South China Craton: Implications for global Lomagundi event. *Geoscience Frontiers*, 13, 101409.
- Luo, G., Ono, S., Beukes, N. J., Wang, D. T., Xie, S., & Summons, R. E. (2016). Rapid oxygenation of Earth's atmosphere 2.33 billion years ago. *Science Advances*, 2, e1600134.
- Lyons, T. W., Reinhard, C. T., & Planavsky, N. J. (2014). The rise of oxygen in Earth's early ocean and atmosphere. *Nature*, 506, 307–315.
- Martin, A. P., Condon, D. J., Prave, A. R., & Lepland, A. (2013). A review of temporal constraints for the Palaeoproterozoic large, positive carbonate carbon isotope excursion (the Lomagundi-Jatuli Event). *Earth Science Reviews*, 127, 242–261.
- Martin, A. P., Condon, D. J., Prave, A. R., Melezhik, V. A., Lepland, A., & Fallick, A. E. (2013). Dating the termination of the Palaeoproterozoic Lomagundi-Jatuli carbon isotopic event in the North Transfennoscandian Greenstone Belt. *Precambrian Research*, 224, 160–168.
- Master, S., Bekker, A., & Karhu, J. A. (2013). Paleoproterozoic high  $\delta^{13}\text{C}_{\text{carb}}$  marbles from the Ruwenzori Mountains, Uganda: Implications for the age of the Buganda Group. *Chemical Geology*, 362, 157–164.
- Melezhik, V. A., & Fallick, A. E. (1996). A widespread positive  $\delta^{13}\text{C}_{\text{carb}}$  anomaly at around 2.33–2.06 Ga on the Fennoscandian Shield: A paradox? *Terra Nova*, 8, 141–157.
- Melezhik, V. A., & Fallick, A. E. (2010). On the Lomagundi-Jatuli carbon isotopic event: The evidence from the Kalix Greenstone Belt, Sweden. *Precambrian Research*, 179, 165–190.
- Melezhik, V. A., Fallick, A. E., Brasier, A. T., & Lepland, A. (2015). Carbonate deposition in the Palaeoproterozoic Onega basin from Fennoscandia: A spotlight on the transition from the Lomagundi-Jatuli to Shunga events. *Earth-Science Reviews*, 147, 65–98.
- Melezhik, V. A., Fallick, A. E., & Clark, T. (1997). Two billion year old isotopically heavy carbon: Evidence from Labrador Trough, Canada. *Canadian Journal of Earth Sciences*, 34, 271–285.
- Melezhik, V. A., Fallick, A. E., & Kuznetsov, A. B. (2005). Palaeoproterozoic, rift-related,  $^{13}\text{C}$ -rich, lacustrine carbonates, NW Russia. Part II: Global isotope signal recorded in the lacustrine dolostones. *Transactions of the Royal Society of Edinburgh: Earth Sciences*, 95, 423–444.
- Melezhik, V. A., Fallick, A. E., Martin, A. P., Condon, D. J., Kump, L. R., Brasier, A. T., & Salminen, P. (2013). 7.3 the Palaeoproterozoic perturbation of the global carbon cycle: The Lomagundi-Jatuli isotopic

- event. In V. Melezhik, A. Prave, A. Fallick, E. Hanski, A. Lepland, L. Kump, & H. Strauss (Eds.), *Reading the archive of earth's oxygenation. Volume 3: Global events and the Fennoscandian Arctic Russia – drilling early earth project* (pp. 1111–1150). Springer.
- Melezhik, V. A., Fallick, A. E., Medvedev, P. V., & Makarikhin, V. V. (1999). Extreme  $\delta^{13}\text{C}_{\text{carb}}$  enrichment in ca. 2.0 Ga magnesite–stromatolite–dolomite–‘red beds’ association in a global context: A case for the world-wide signal enhanced by a local environment. *Earth-Science Reviews*, 48, 71–120.
- Melezhik, V. A., Fallick, A. E., Smirnov, Y. P., & Yakovlev, Y. N. (2003). Fractionation of carbon and oxygen isotopes in  $^{13}\text{C}$ -rich Palaeoproterozoic dolostones in the transition from medium-grade to high-grade greenschist facies: A case study from the Kola Superdeep Drillhole. *Journal of the Geological Society*, 160, 71–82.
- Melezhik, V. A., Huhma, H., Condon, D. J., Fallick, A. E., & Whitehouse, M. J. (2007). Temporal constraints on the Paleoproterozoic Lomagundi–Jatuli carbon isotopic event. *Geology*, 35, 655–658.
- Mirota, M. D., & Veizer, J. (1994). Geochemistry of precambrian carbonates: VI. Aphelian Alبان Formations, Quebec, Canada. *Geochimica et Cosmochimica Acta*, 58, 1735–1745.
- Niiranen, T., Hanski, E., & Eilu, P. (2003). General geology, alteration, and iron deposits in the Palaeoproterozoic Misi region, northern Finland. *Bulletin of the Geological Society of Finland*, 75, 69–92.
- Ossa Ossa, F., Eickmann, B., Hofmann, A., Planavsky, N. J., Asael, D., Pambo, F., & Bekker, A. (2018). Two-step deoxygenation at the end of the Paleoproterozoic Lomagundi event. *Earth and Planetary Science Letters*, 486, 70–83.
- Poulton, S. W., Bekker, A., Cumming, V. M., Zerkle, A. L., Canfield, D. E., & Johnston, D. T. (2021). A 200-million-year delay in permanent atmospheric oxygenation. *Nature*, 592, 232–236.
- Prave, A. R., Kirsämäe, K., Lepland, A., Fallick, A. E., Kreitsmann, T., Deines, Y. E., Romashkin, A. E., Rychanchik, D. V., Medvedev, P. V., Moussavou, M., Bakakas, K., & Hodgeskiss, M. S. W. (2022). The grandest of them all: The Lomagundi–Jatuli Event and Earth’s oxygenation. *Journal of the Geological Society*, 179(1), jgs2021-036.
- Préat, A., Bouton, P., Thieblemont, D., Prian, J.-P., Ndounze, S. S., & Delpomord, F. (2011). Paleoproterozoic high  $\delta^{13}\text{C}$  dolomites from the Lastoursville and Franceville basins (SE Gabon): Stratigraphic and synsedimentary subsidence implications. *Precambrian Research*, 189, 212–228.
- Purohit, R., Sanyal, P., Roy, A. B., & Bhattacharya, S. K. (2010).  $^{13}\text{C}$  enrichment in the Palaeoproterozoic carbonate rocks of Aravalli Supergroup, Northwest India: Influence of depositional environment. *Gondwana Research*, 18, 538–546.
- Salminen, P. E., Karhu, J. A., & Melezhik, V. A. (2013). Tracking lateral  $\delta^{13}\text{C}_{\text{carb}}$  variation in the Paleoproterozoic Pechenga Greenstone Belt, the north eastern Fennoscandian Shield. *Precambrian Research*, 228, 177–193.
- Santos, R. V., Santos, E. J., Neto, J. A. S., Carmona, L. C. M., Sial, A. N., Mancini, L. H., Santos, L. C. M. L., Nascimento, G. H., Mendes, L. U. S., & Anastácio, E. M. F. (2013). Isotope geochemistry of Paleoproterozoic metacarbonates from Itatuba, Borborema Province, Northeastern Brazil: Evidence of marble melting within a collisional suture. *Gondwana Research*, 23, 380–389.
- Schidlowski, M., Eichmann, R., & Junge, C. E. (1975). Precambrian sedimentary carbonates: Carbon and oxygen isotope geochemistry and implications for the terrestrial oxygen budget. *Precambrian Research*, 2, 1–69.
- Schidlowski, M., Eichmann, R., & Junge, C. E. (1976). Carbon isotope geochemistry of the Precambrian Lomagundi carbonate province, Rhodesia. *Geochimica et Cosmochimica Acta*, 40, 449–455.
- Schidlowski, M., Hayes, J. M., & Kaplan, I. R. (1983). Isotopic inferences of ancient biochemistries: Carbon, hydrogen and nitrogen. In J. W. Schopf (Ed.), *Earth’s earliest biosphere: Its origin and evolution* (pp. 149–186). Princeton University Press.
- Schröder, S., Bekker, A., Beukes, N. J., Strauss, H., & Van Niekerk, H. S. (2008). Rise in seawater sulphate concentration associated with the Paleoproterozoic positive carbon isotope excursion: Evidence from sulphate evaporites in the ~2.2–2.1 Gyr shallow-marine Lucknow formation, South Africa. *Terra Nova*, 20, 108–117.
- Schröder, S., Beukes, N. J., & Armstrong, R. A. (2016). Detrital zircon constraints on the tectonostratigraphy of the Paleoproterozoic Pretoria Group, South Africa. *Precambrian Research*, 278, 362–393.
- Shen, J., Algeo, T. J., Hu, Q., Zhang, N., Zhou, L., Xia, W., Xie, S., & Feng, Q. (2012). Negative C-isotope excursions at the Permian-Triassic boundary linked to volcanism. *Geology*, 40(11), 963–966.
- Tang, H. S., Chen, Y. J., Wu, G., & Lai, Y. (2008). The C-O isotope composition of the Liaohe Group, northern Liaoning province and its geologic implications. *Acta Petrologica Sinica*, 24, 129–138. (in Chinese with English abstract).
- Tang, H. S., Chen, Y. J., Wu, G., & Lai, Y. (2011). Paleoproterozoic positive  $\delta^{13}\text{C}_{\text{carb}}$  excursion in the northeastern Sino-Korean craton: Evidence of the Lomagundi Event. *Gondwana Research*, 19, 471–481.
- Xu, W. Q., Li, Z. Y., Liu, Y. H., Liu, Z. Y., & Ma, Z. L. (1997). Preliminary discussion on the establishment of Proterozoic stratigraphic framework of Fanhe area, Tieling. *Liaoning Geology*, 14(1), 30–39. (in Chinese with English abstract).
- Yang, J., Zeng, Z. X., Cai, X. F., Li, Z. Y., Li, T. B., Meng, F., & He, W. J. (2013). Carbon and oxygen isotopes analyses for the Sinian carbonates in the Helan Mountain, North China. *Chinese Science Bulletin*, 58, 3943–3955.

## SUPPORTING INFORMATION

Additional supporting information can be found online in the Supporting Information section at the end of this article.

### Appendix S1.

**How to cite this article:** Zhang, S.-H., Wang, H.-Y., Tang, H.-S., Cai, Y.-H., Kong, L.-H., Pei, J.-L., Zhang, Q.-Q., Hu, G.-H., & Zhao, Y. (2024). High positive carbonate carbon isotope excursion identified in the North China Craton: Implications for the Lomagundi–Jatuli Event. *Terra Nova*, 36, 25–36. <https://doi.org/10.1111/ter.12687>